

Supporting Information

Fine-tuning of Inner Sidechain of Donor Polymer for Efficient Indoor Organic Photovoltaics

Sang Hyeon Kim,^a Cheng Sun,^b Muhammad Ahsan Saeed,^a Hyeok-Jin Kwon,^c Tae Hyuk Kim,^a Soon-Ki Kwon,^d Yun-Hi Kim^{*b} and Jae Won Shim^{*a}

^aSchool of Electrical Engineering, Korea University, Seoul 02841, Republic of Korea

^bDepartment of Chemistry & RINS, Gyeongsang National University, Jinju 52828, Republic of Korea

^cDepartment of Chemical Engineering, Pohang University of Science and Technology, Pohang 37673, Republic of Korea

^dDepartment of Materials Engineering and Convergence Technology and ERI, Gyeongsang National University, Jinju 52828, Republic of Korea

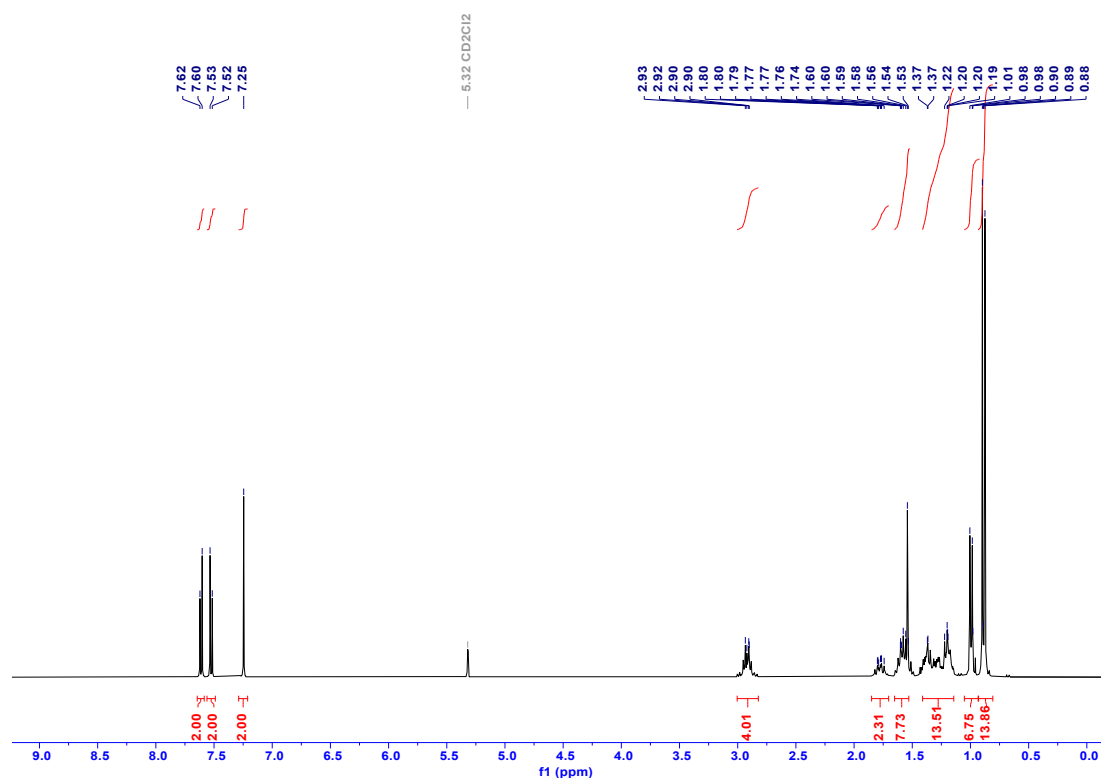
Corresponding authors: ykim@gnu.ac.kr (*Y.H. Kim*) jwshim19@korea.ac.kr (*J.W. Shim*)

Materials

All solvents and reagents were purchased from Sigma-Aldrich. All other materials were of a common commercial level and were used as received. All solvents used were purified prior to use. BDD and PBDB-EH-3Cl was synthesized following the previous literature. [S0]

Measurements

$^1\text{H-NMR}$ and $^{13}\text{C-NMR}$ were recorded with a Bruker DRX-300 and Avance 500 spectrometer, respectively. Mass spectra were recorded on a JEOL JMS-700 spectrometer. Thermal gravimetric analysis (TGA) was performed on a TA TGA 2100 thermogravimetric analyzer under nitrogen atmosphere with a heating rate of $10\text{ }^\circ\text{C}/\text{min}$. Differential scanning calorimetry (DSC) was conducted under nitrogen on a TA Instruments 2100 DSC. The sample was heated at $10\text{ }^\circ\text{C}/\text{min}$ from 30 to $300\text{ }^\circ\text{C}$. The UV-Vis absorption spectra were determined using a Cary 5000 UV-vis-near-IR double beam spectrophotometer. Cyclic voltammetry (CV) was performed using a PowerLab/AD instrument model system in a 0.1 M tetrabutylammonium hexafluorophosphate (Bu_4NPF_6) solution in anhydrous acetonitrile as the supporting electrolyte, at a scan rate of 100 mV/s . A glassy carbon electrode was used as the working electrode. A platinum wire was used as the counter electrode, and an Ag/AgCl electrode was used as the reference electrode.



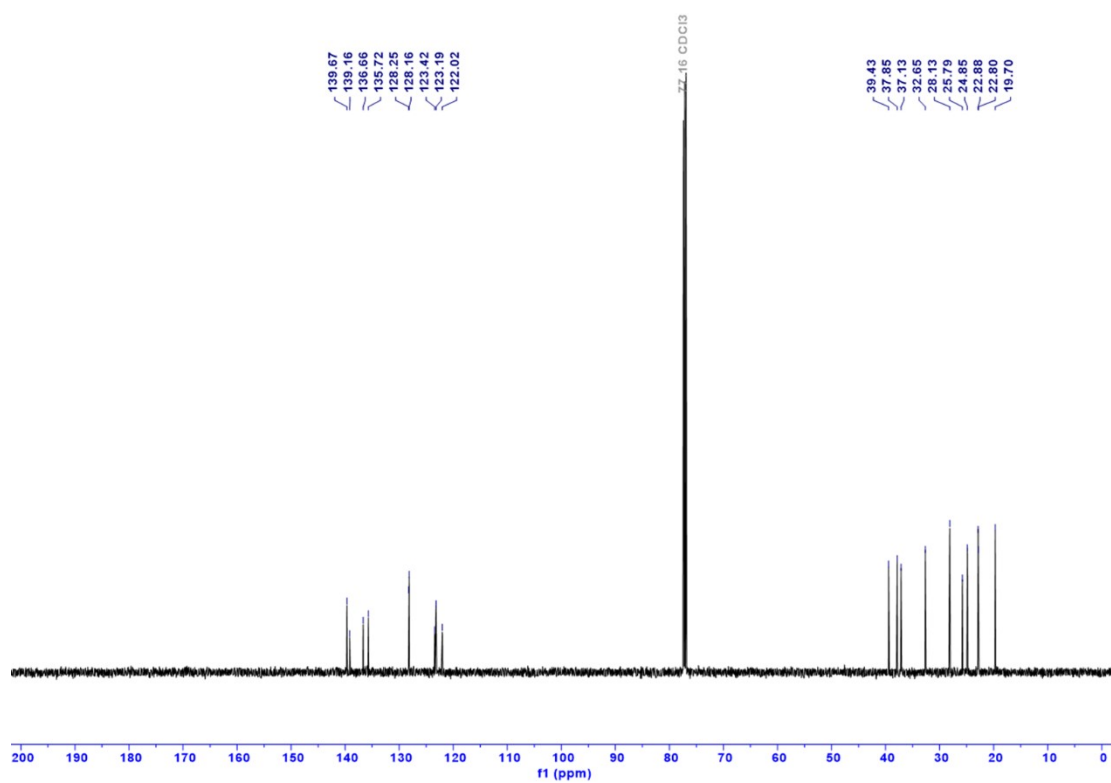


Figure S1. ^1H NMR and ^{13}C NMR spectra of DMO-3-Cl-BDT.

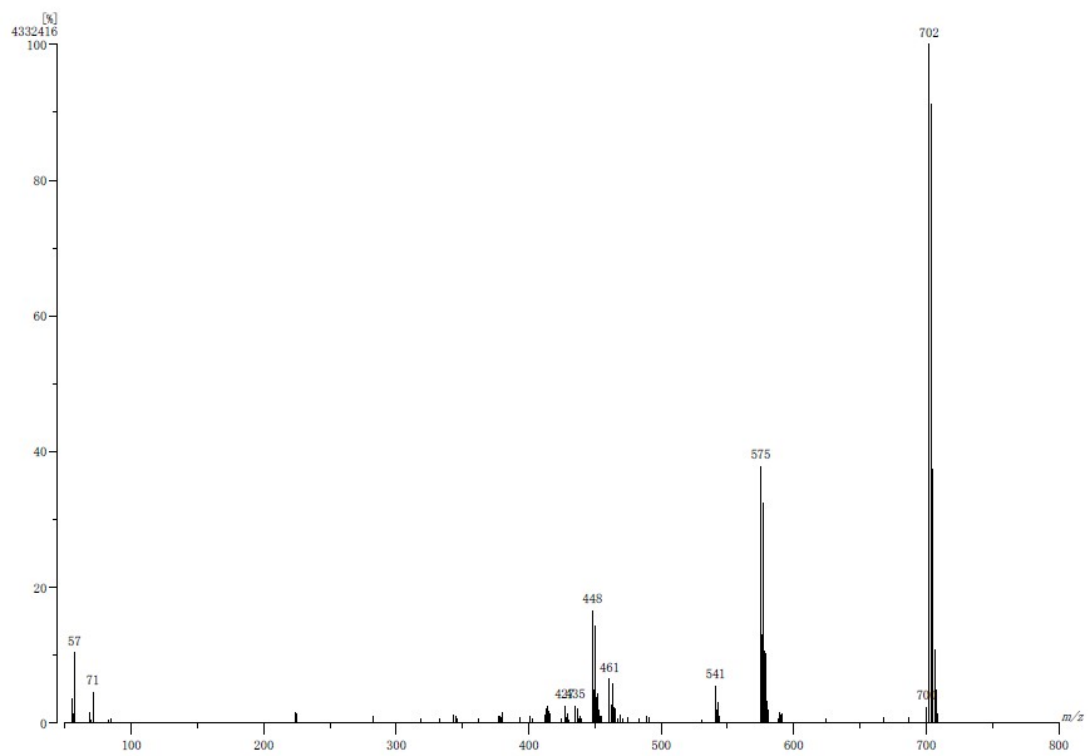


Figure S2. HR-mass spectra of DMO-3-Cl-BDT.

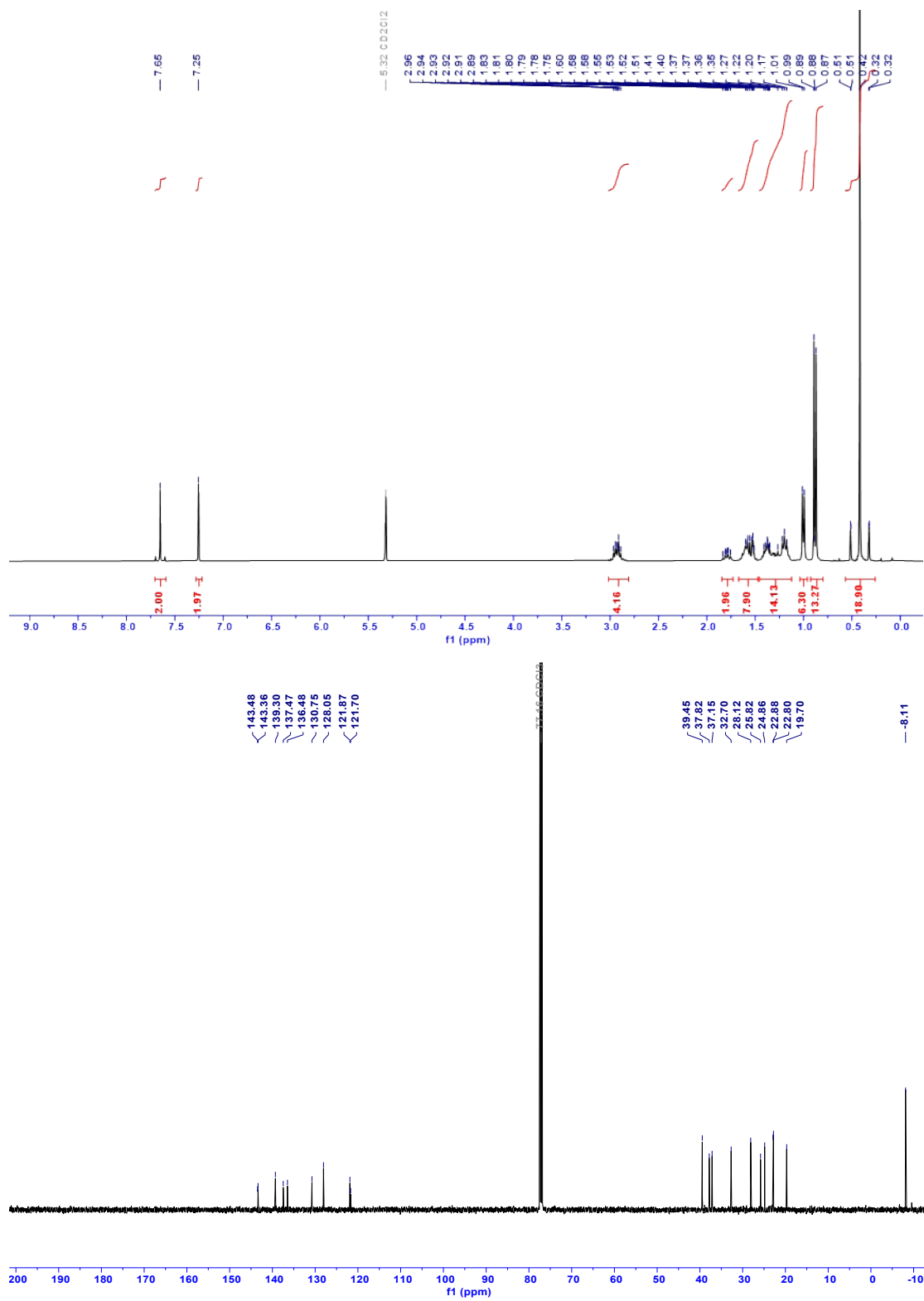


Figure S3. ^1H NMR and ^{13}C NMR spectra of DMO-3Cl-BDT-Sn.

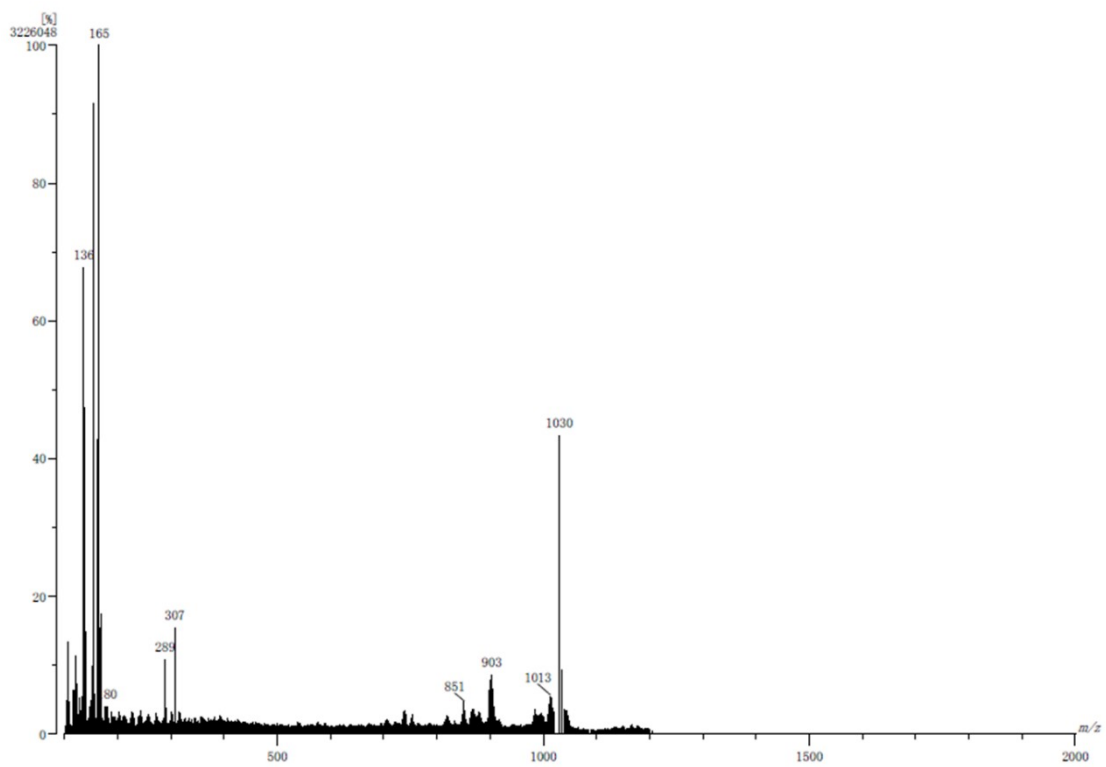


Figure S4. HR-mass spectra of DMO-3Cl-BDT-Sn

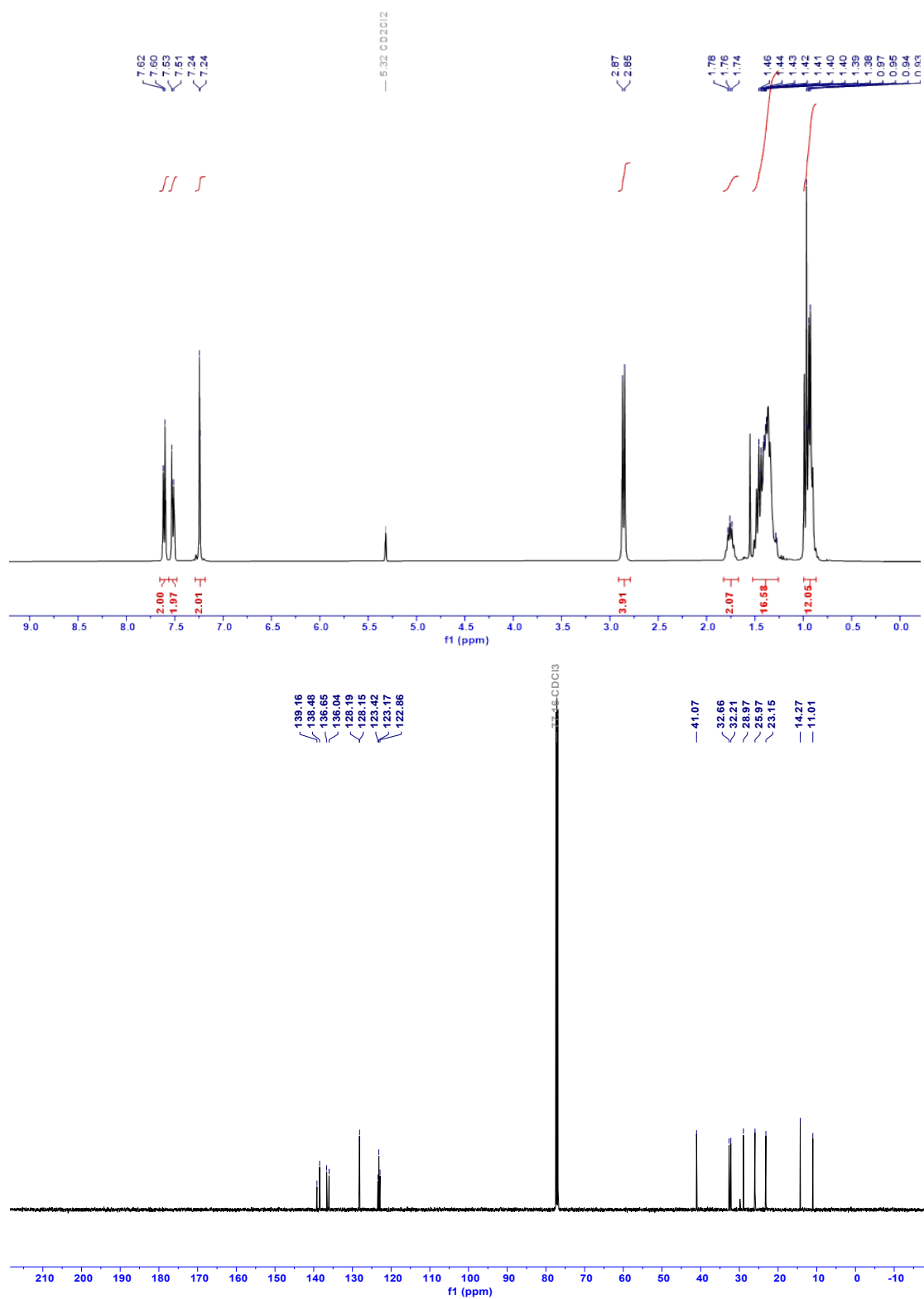


Figure S5. ^1H NMR and ^{13}C NMR spectra of EH-4Cl-BDT.

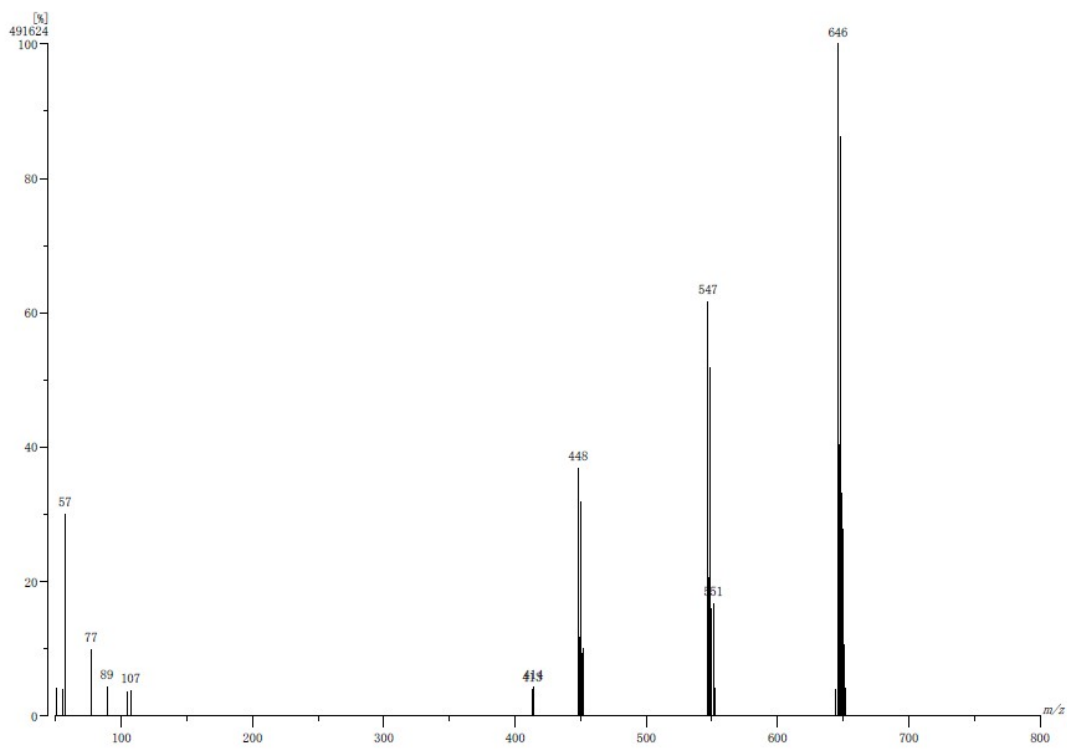


Figure S6. HR-mass spectra of EH-4Cl-BDT.

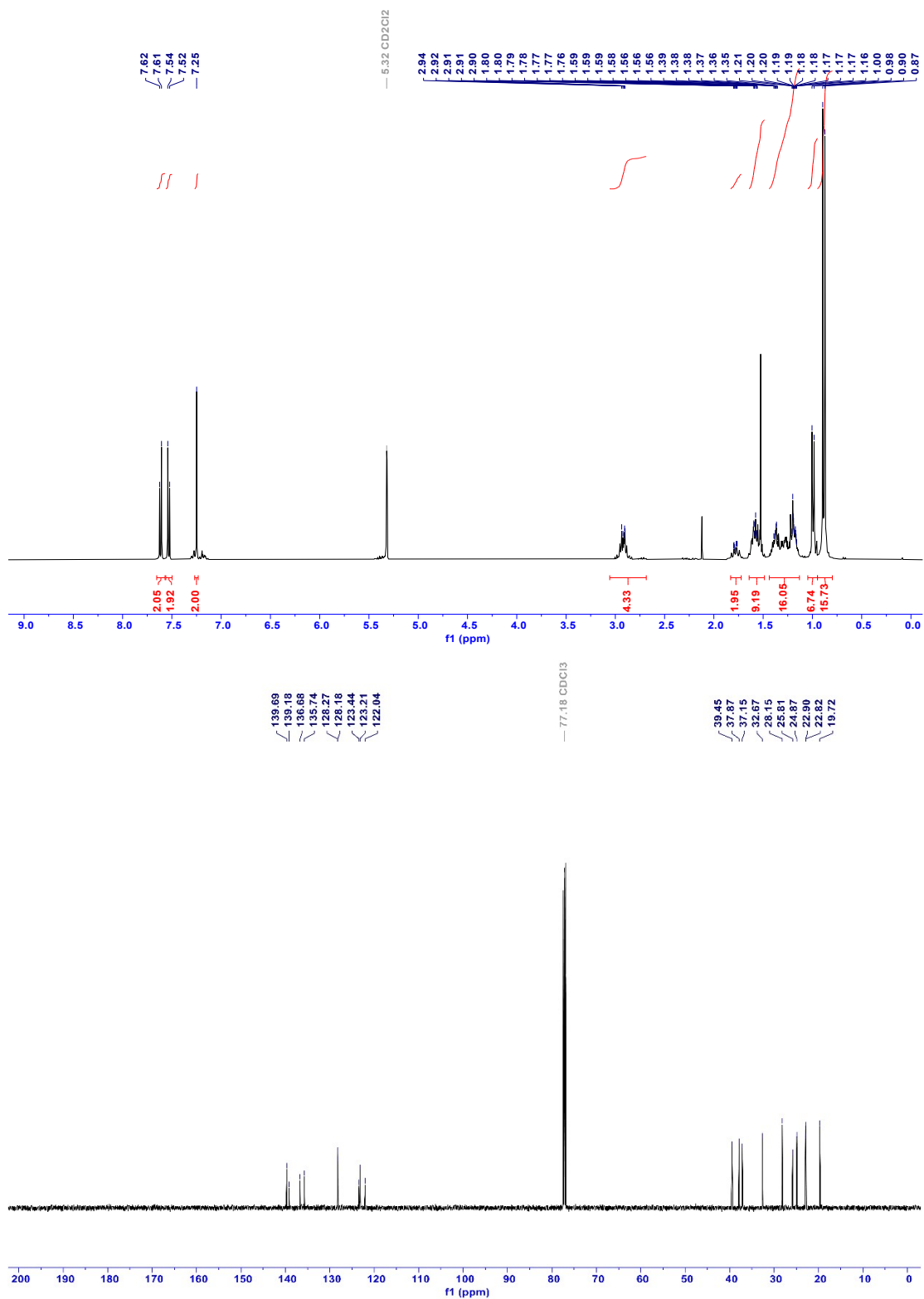


Figure S7. ¹H NMR and ¹³C NMR spectra of DMO-4Cl-BDT.

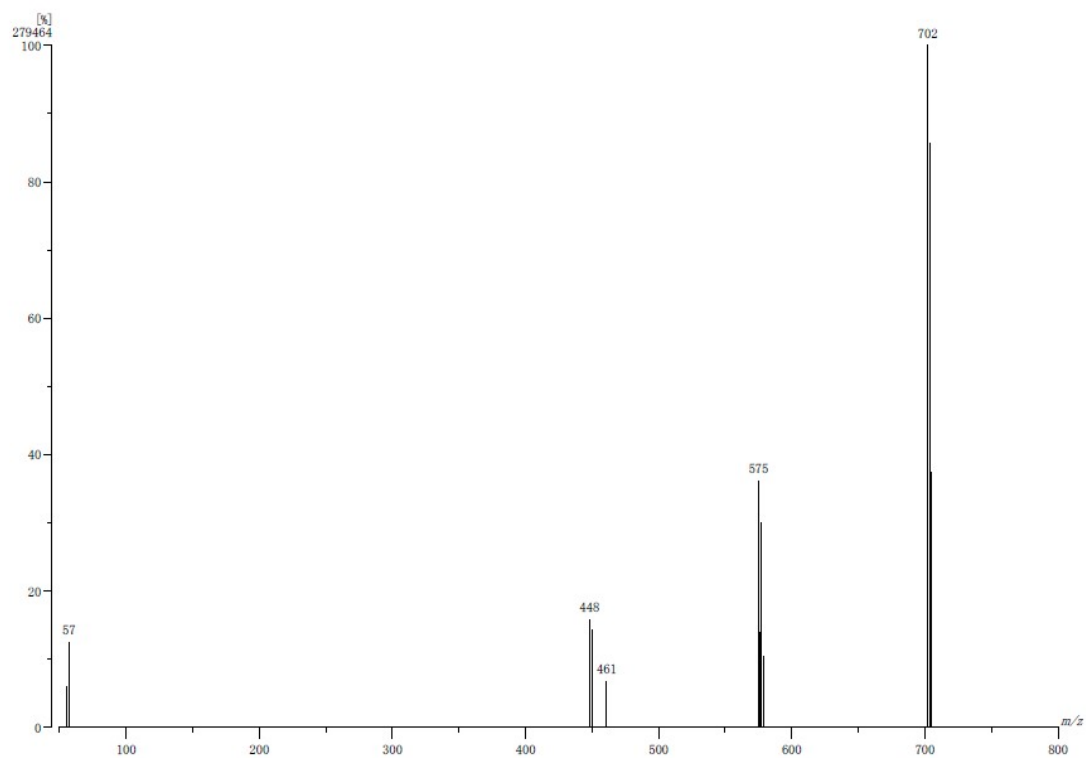


Figure S8. HR-mass spectra of DMO-4Cl-BDT.

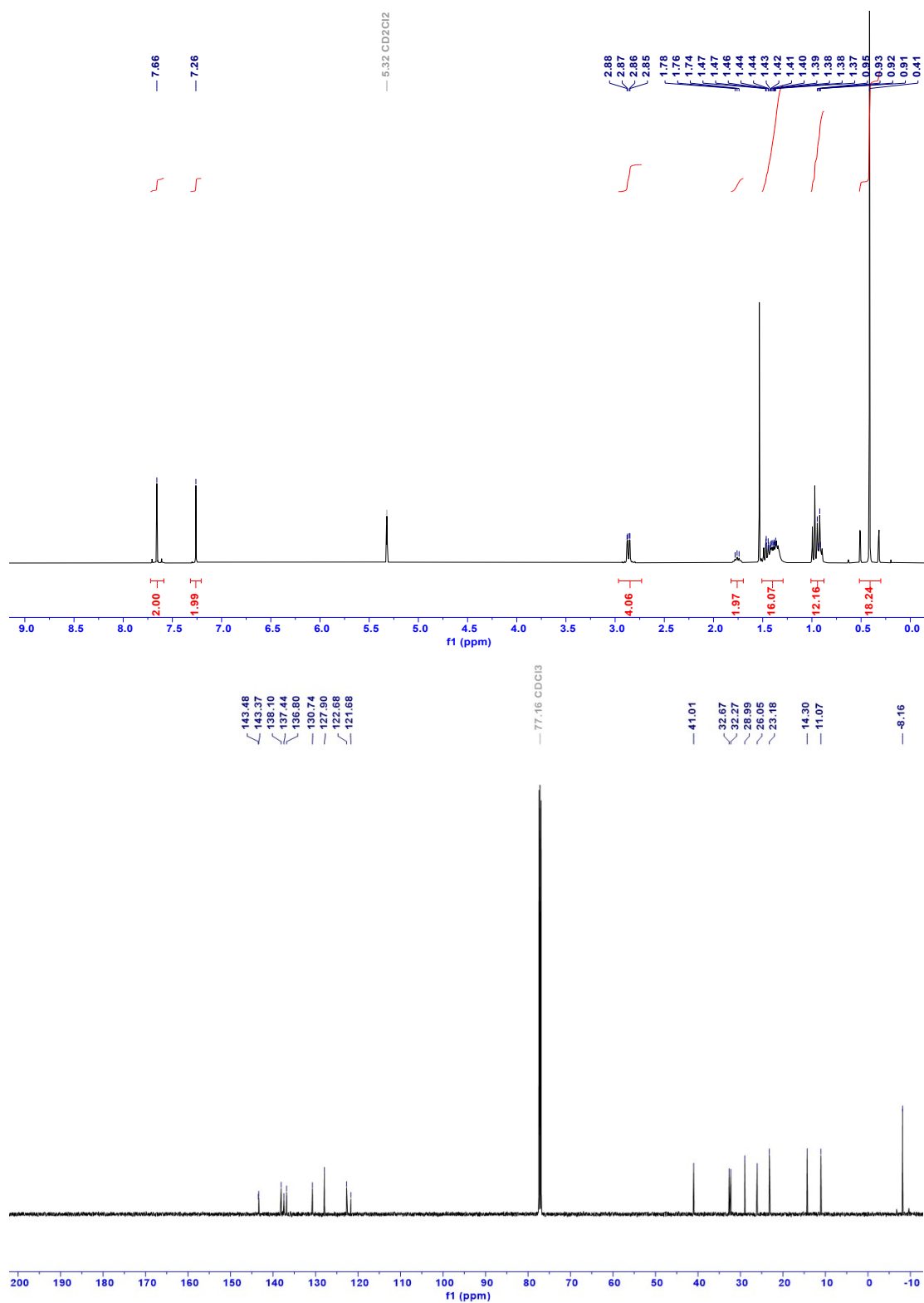


Figure S9. ¹H NMR and ¹³C NMR spectra of EH-4Cl-BDT-Sn.

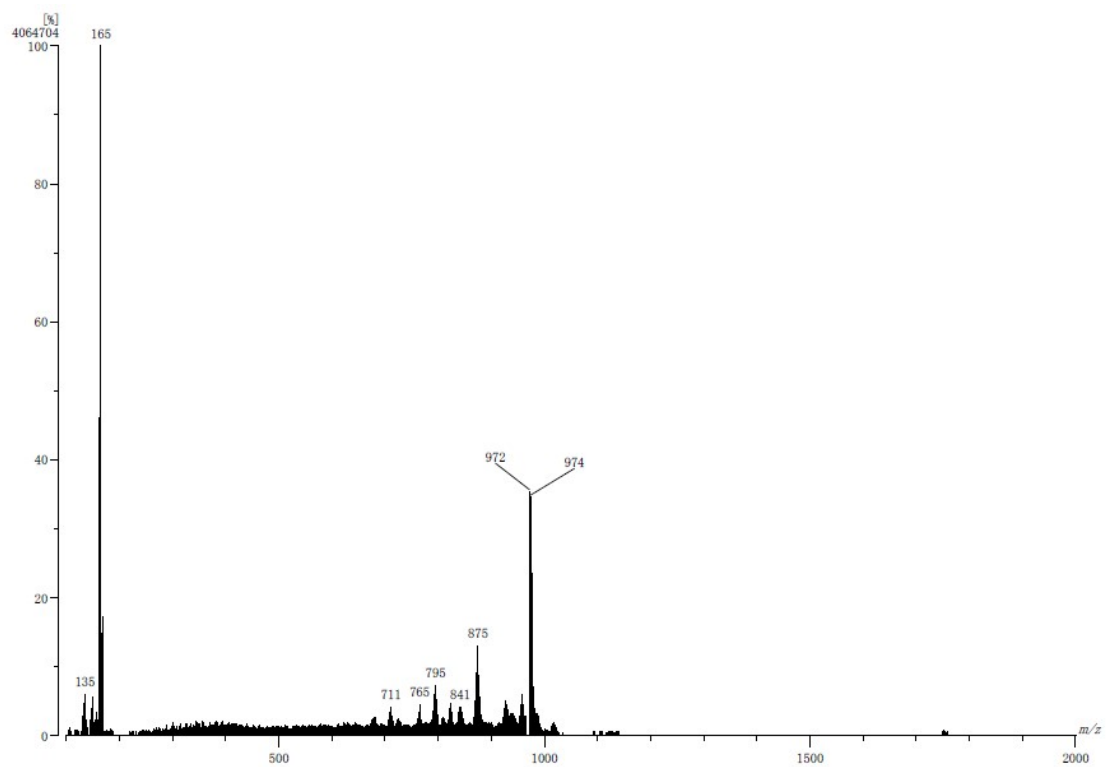


Figure S10. HR-mass spectra of EH-4Cl-BDT-Sn.

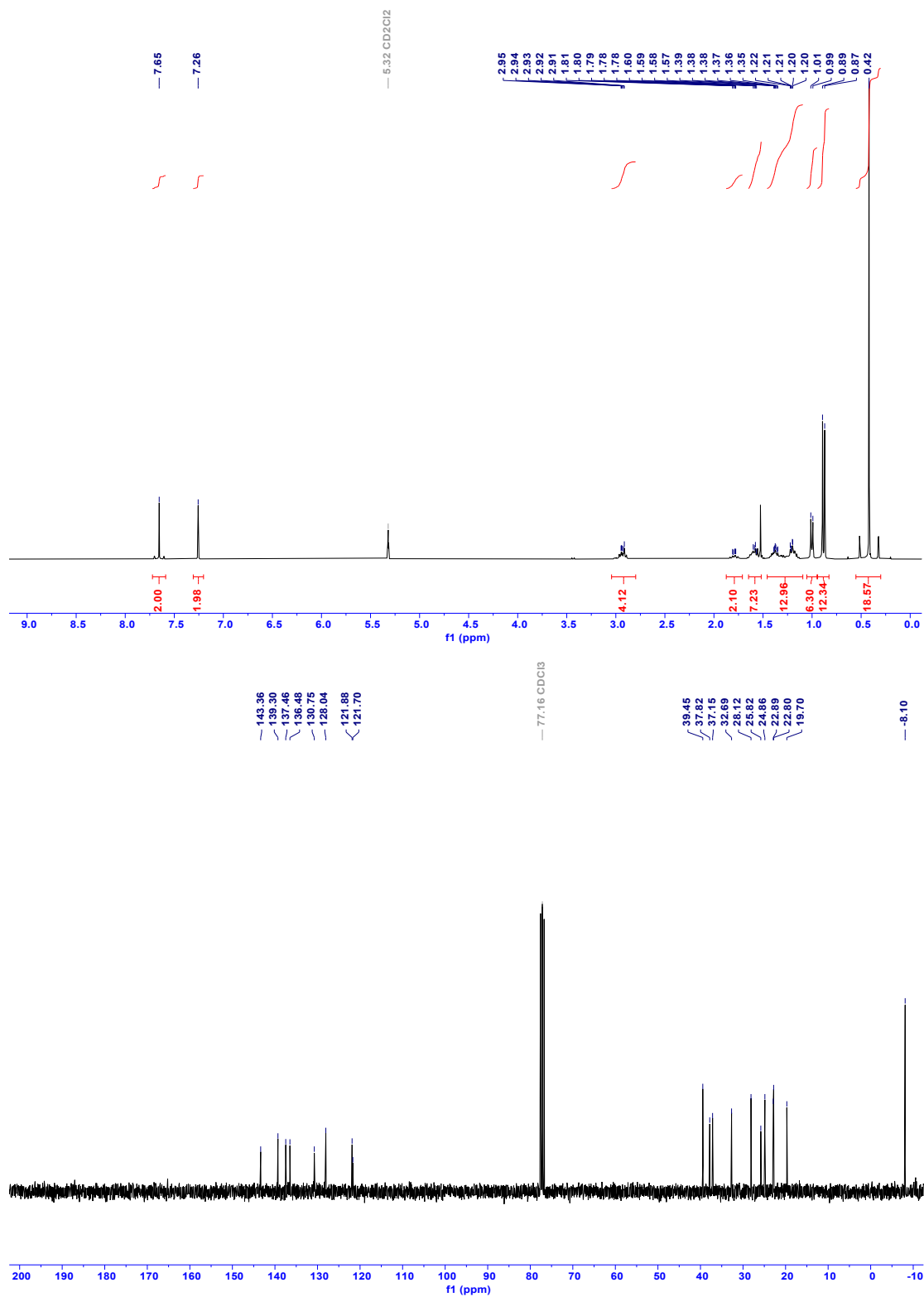


Figure S11. ¹H NMR and ¹³C NMR spectra of DMO-4Cl-BDT-Sn.

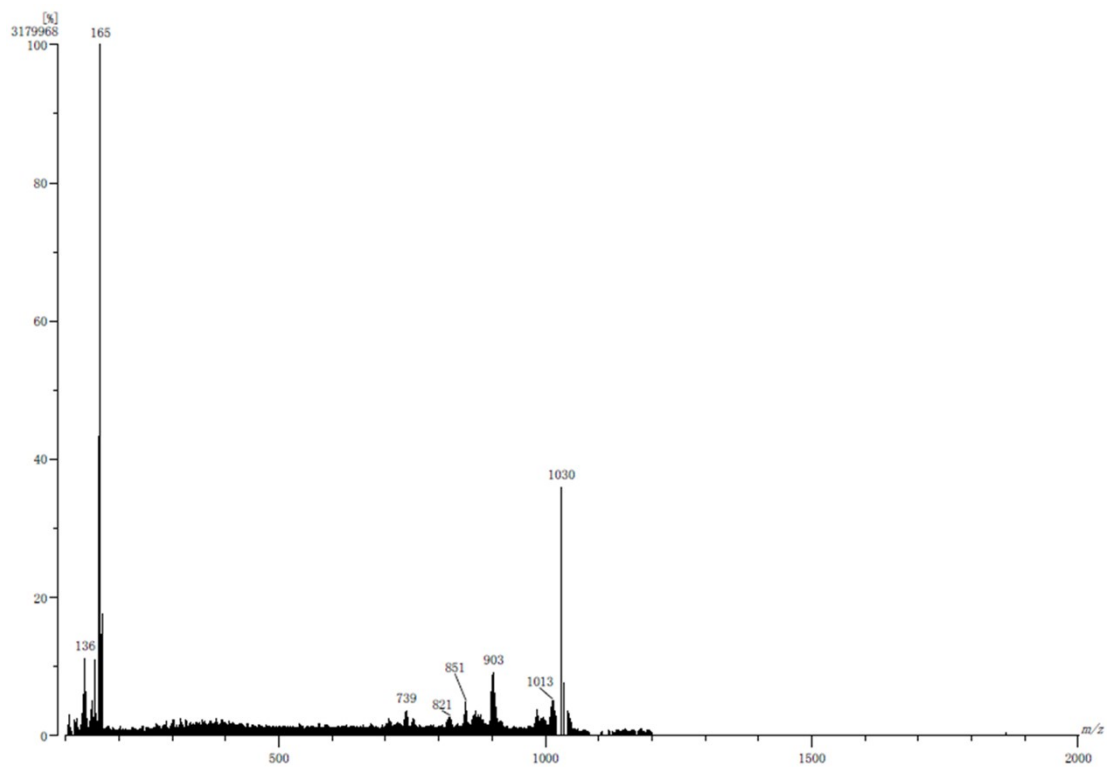


Figure S12. HR-mass spectra of DMO-4Cl-BDT-Sn.

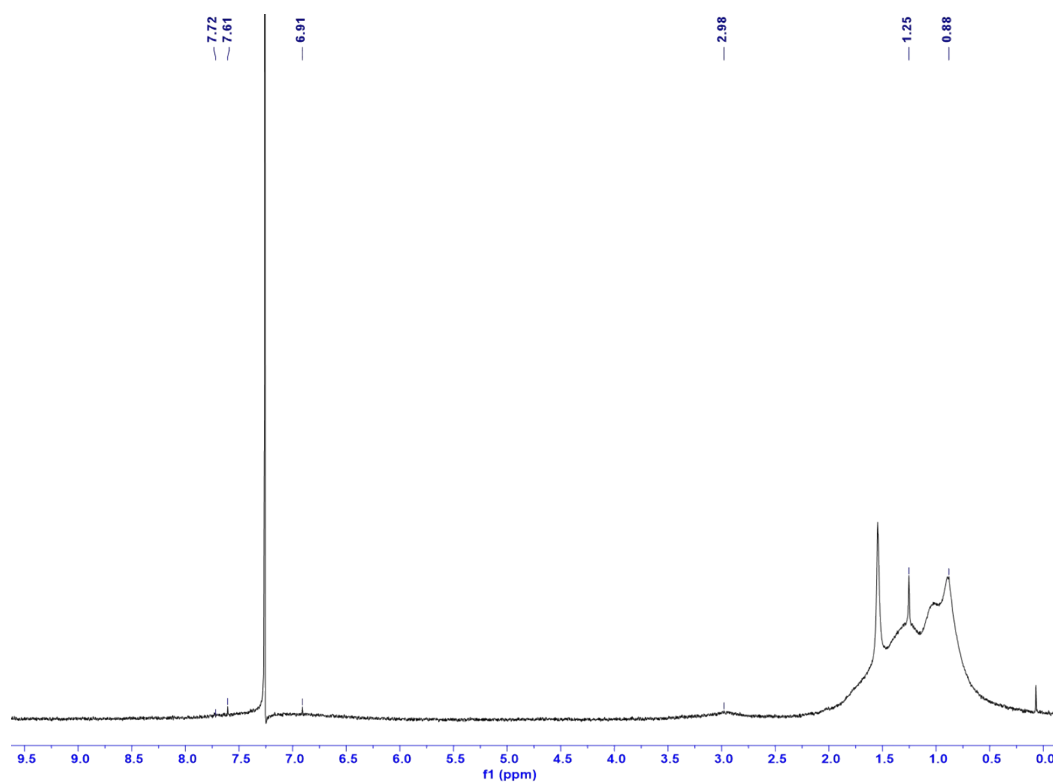


Figure S13. ^1H NMR spectra of PBDB-DMO-3Cl.

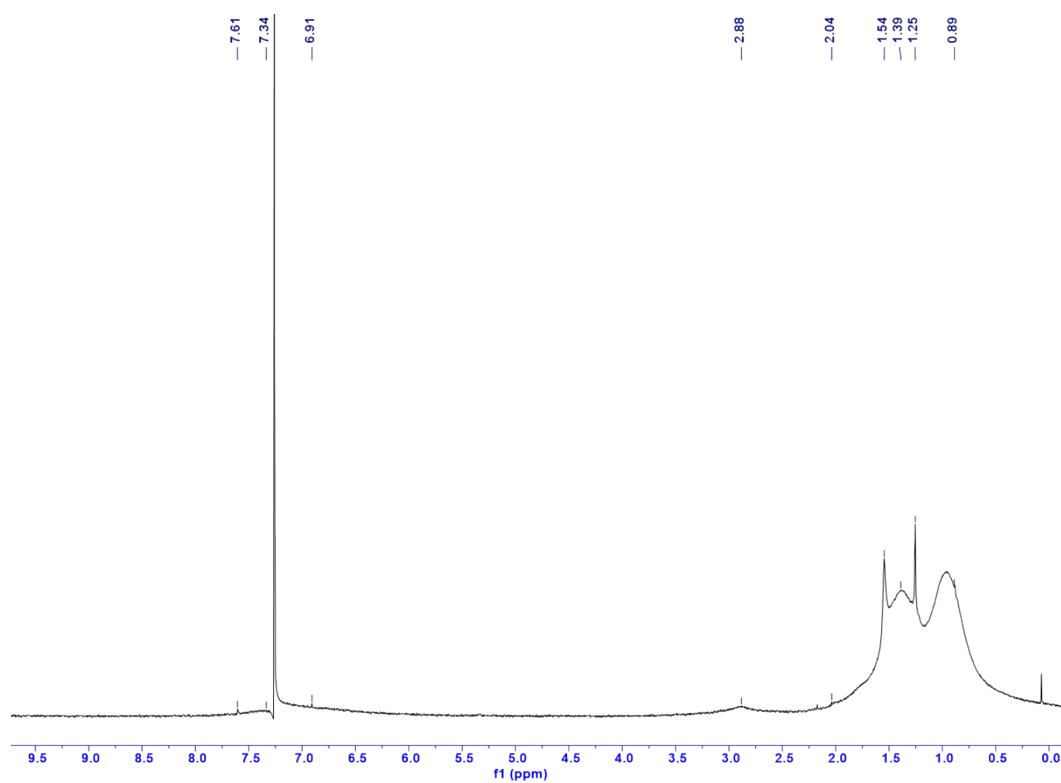


Figure S14. ^1H NMR spectra of PBDB-EH-4Cl.

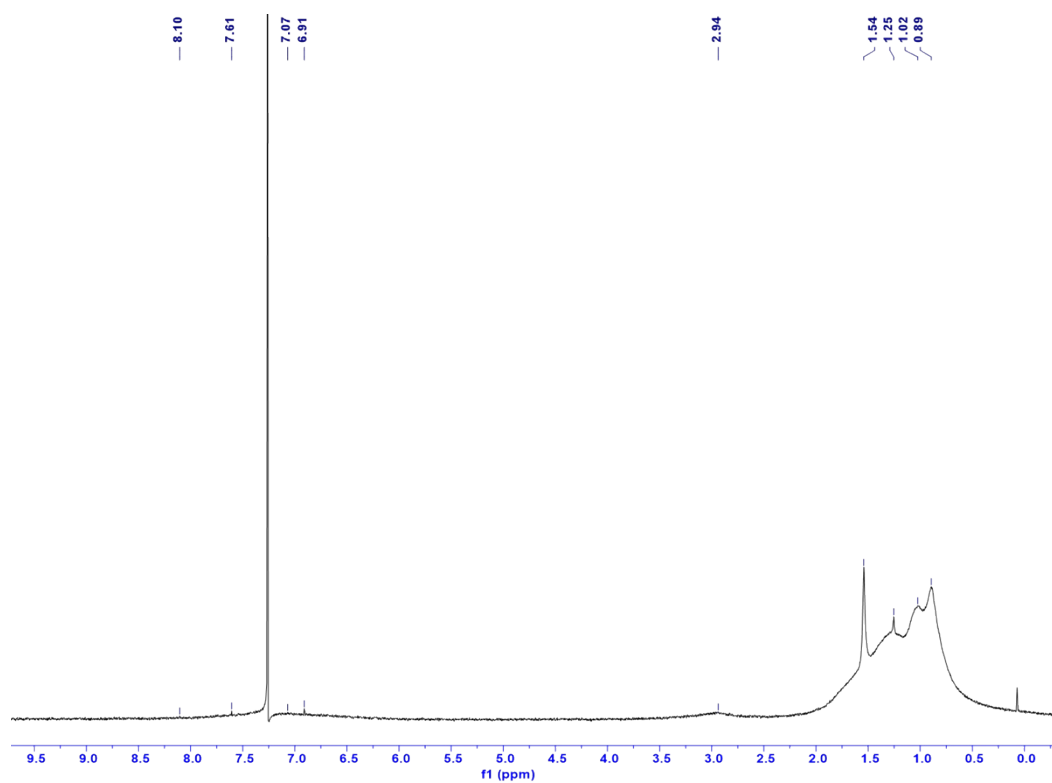


Figure S15. ^1H NMR spectra of PBDB-DMO-4Cl.

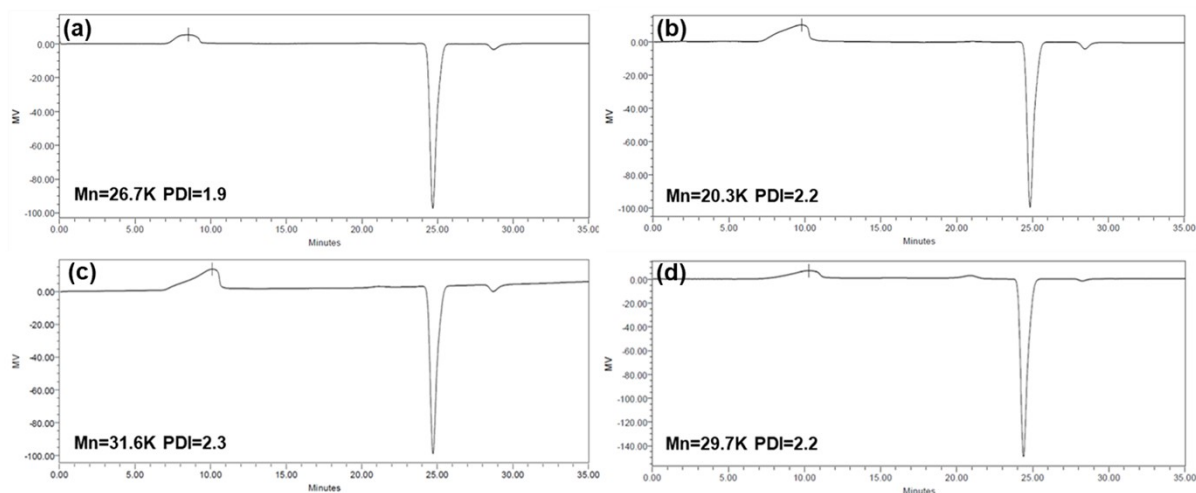


Figure S16. GPC curves of PM7 series polymer (a) PBDB-EH-3Cl (b) PBDB-EH-4Cl (c) PBDB-DMO-3Cl (d) PBDB-DMO-4Cl in chloroform.

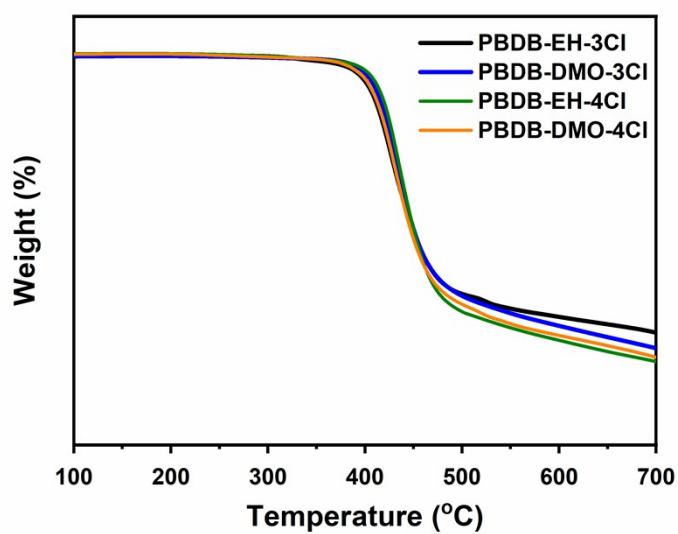


Figure S17. TGA plots of PM7 series polymer with a heating rate of 10 °C/min under the N₂ atmosphere

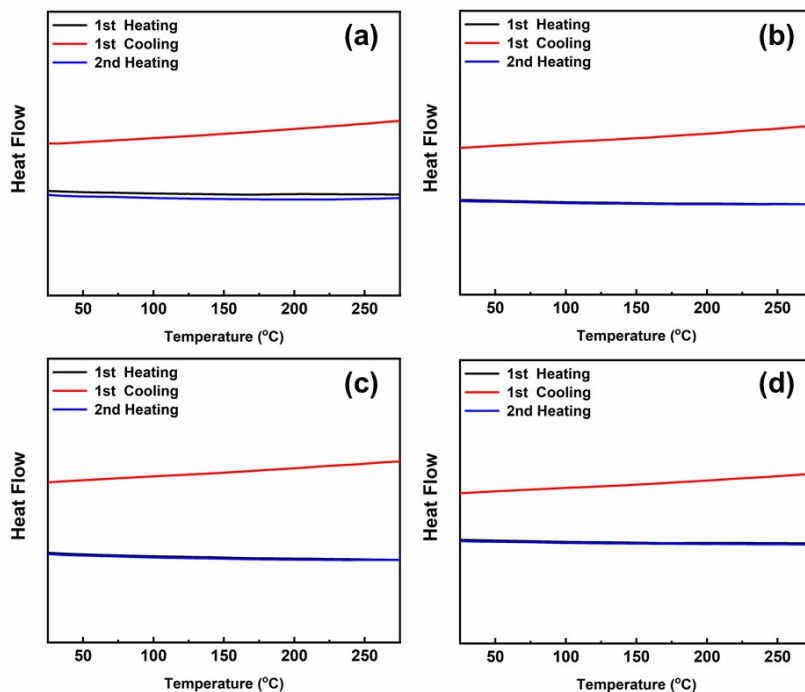


Figure S18. DSC plots of PM7 series polymer donor (a) PBDB-EH-3Cl (b) PBDB-DMO-3Cl (c) PBDB-EH-4Cl (d)PBDB-DMO-4Cl under the N_2 atmosphere

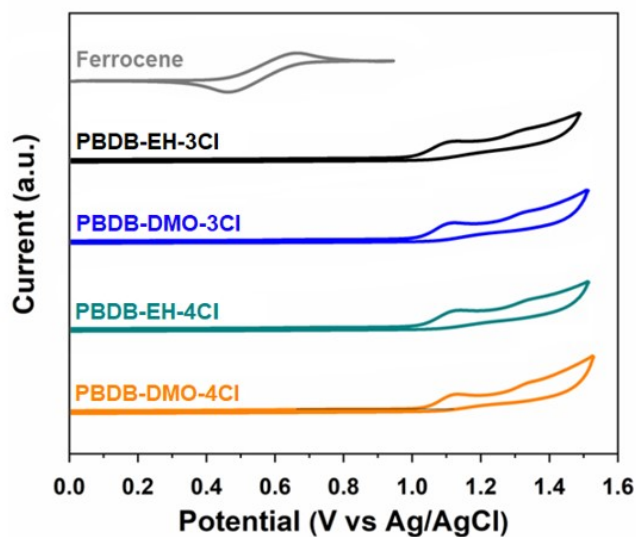


Figure S19. Cyclic voltammetry curves of PM7 series polymer donors

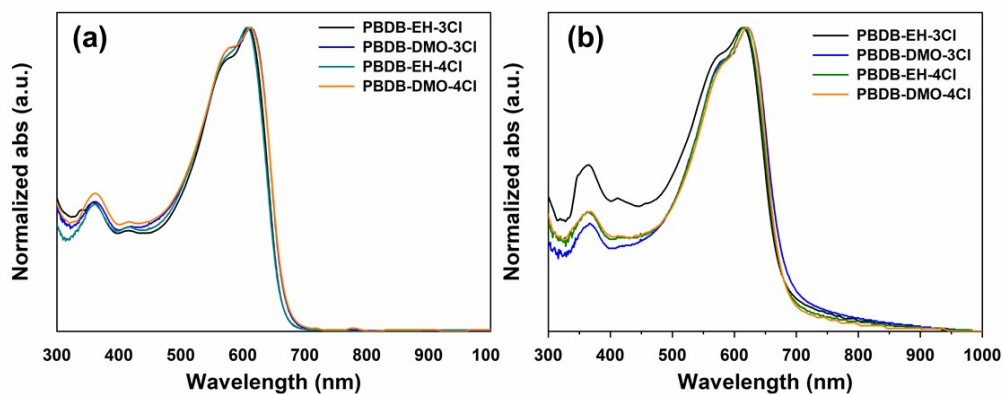


Figure S20. UV-vis absorption spectra of PM7 series polymer donor in chloroform (a) and film (b)

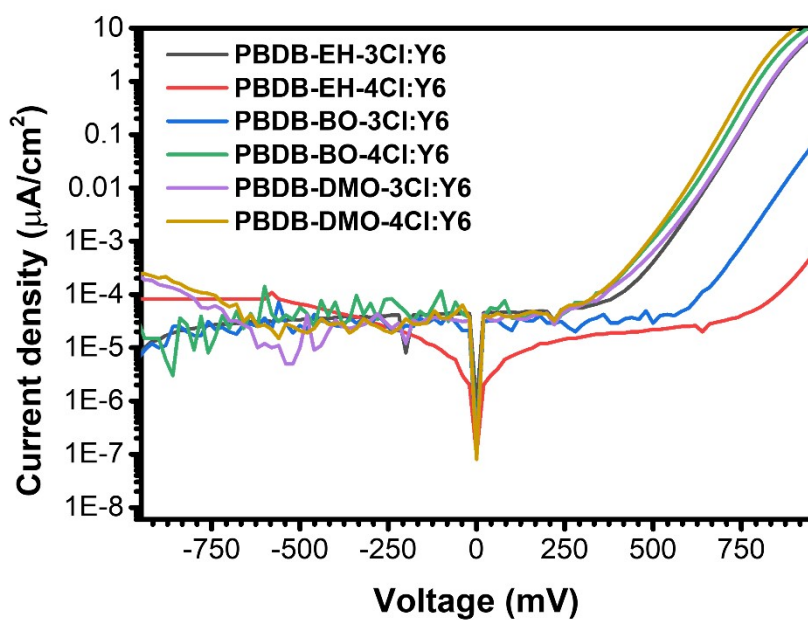


Figure S21. Dark curve of PM7 series polymer donor based OPVs

The performance of the OPVs is often described with a single-diode equivalent circuit model, including one current source and two parasitic resistances, a shunt resistance (R_p) and a series resistance (R_s) under illumination. The R_p is related to the leakage current, recombination, *etc.*, and the R_s is originated from the resistive components of the device such as the resistance of electrodes and bulk resistance of photoactive layers.

By using the Shockley **Eq. 1,2**, the circuit model under illumination can be formulated, and the J_{SC} and the V_{OC} can be expressed as follows,

$$J_{SC} = -\frac{1}{R_s} \left[J_{ph} - J_0 \left(\exp\left(\frac{|J_{SC}| R_s A}{nkT}\right) - 1 \right) \right] \quad (1)$$

$$V_{OC} = \frac{kT}{q} \ln \left\{ 1 + \frac{J_{ph}}{J_0} \left(1 - \frac{V_{OC}}{J_{ph} R_p A} \right) \right\} \approx \frac{kT}{q} \ln \left\{ 1 + \frac{J_{ph}}{J_0} \right\} \quad (2)$$

where J_{ph} is the photo-current density, J_0 is the reverse saturation current density, n is the ideality factor, q is the elementary charge number (1.602×10^{-19} C), k is the Boltzmann constant (8.617×10^{-5} eV/K), T is temperature, and A is the area of the photoactive region. Also, when

$R_p \gg R_s$ and $J_{ph} = J_{SC}$, Eq. (2) can be written as $V_{OC} \approx \frac{kT}{q} \ln \left\{ 1 + \frac{J_{ph}}{J_0} \right\}$, which seems to be independent of R_s and R_p . The $R_s A$ and $R_p A$ values were extracted from the inverse slope of the J - V characteristics under illumination in the range of 0.96 – 1.0 V and near 0 V (close to the J_{SC} point), respectively. The FF ($J_{max} \times V_{max} / J_{SC} \times V_{OC}$) can be shown as a function of the normalized V_{OC} ($v_{OC} = eV_{OC} / nkT$), normalized R_s ($r_s = R_s / R_{CH}$), and normalized R_p ($r_p = R_p / R_{CH}$), where the characteristic resistance (R_{CH}) is defined as $R_{CH} = V_{OC} / (J_{SC} A)$. The equation for the ideal FF₀ of the OPVs is expressed as follows:

$$FF_0 = \frac{v_{OC} - \ln(v_{OC} + 0.72)}{v_{OC} + 1} \quad (3)$$

where, $R_s = 0$ and $R_p = \infty$. However, owing to the parasitic resistance effects, the real FF value should deviate from the ideal FF₀, and thus, semi-empirical expressions with the parasitic effects are shown below:

$$FF_s = FF_0 (1 - 1.1r_s) + 0.19r_s^2, \quad (0 \leq r_s \leq 0.4, 1/r_p = 0) \quad (4)$$

and,

$$FF_{SP} = FF_s \left\{ 1 - \frac{(v_{OC} + 0.7) FF_s}{v_{OC} r_p} \right\}, \quad (0 \leq r_s + 1/r_p \leq 0.4) \quad (5).$$

$$V_{OC} = \frac{E_{gap}}{q} - \frac{kT}{q} \ln \left\{ \frac{(1 - P_D) \gamma N_C^2}{P_D G} \right\} \quad (6)$$

where E_{gap} is the energy difference between the HOMO-donor and LUMO-acceptor, q is the elementary charge, k is the Boltzmann constant, T is the temperature in Kelvin, P_D is the dissociation probability of the electron (e)-hole (h) pairs, γ is the Langevin recombination constant, N_C is the effective density of states, and G is the generation rate of bound e-h pairs.

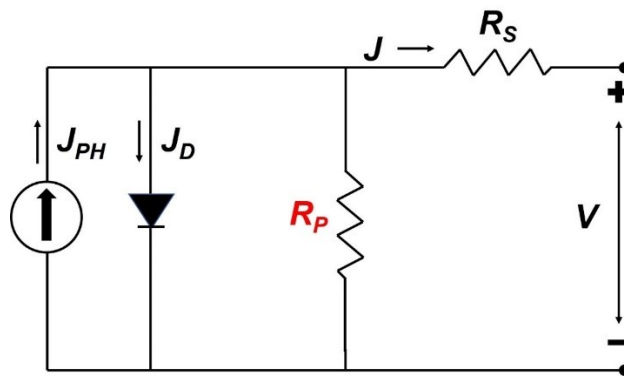


Fig. S22. Parasitic resistance effects based on the single-diode equivalent circuit model.

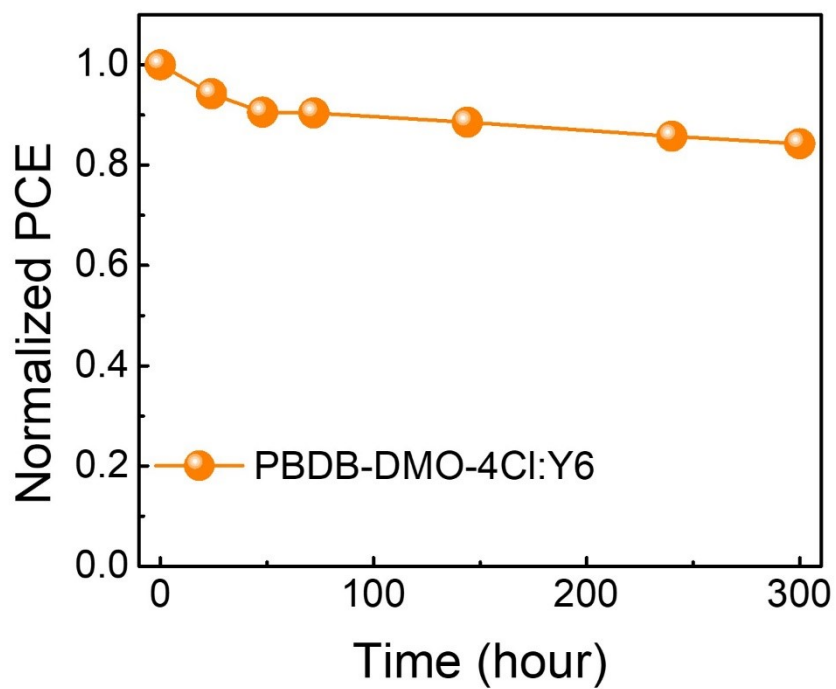
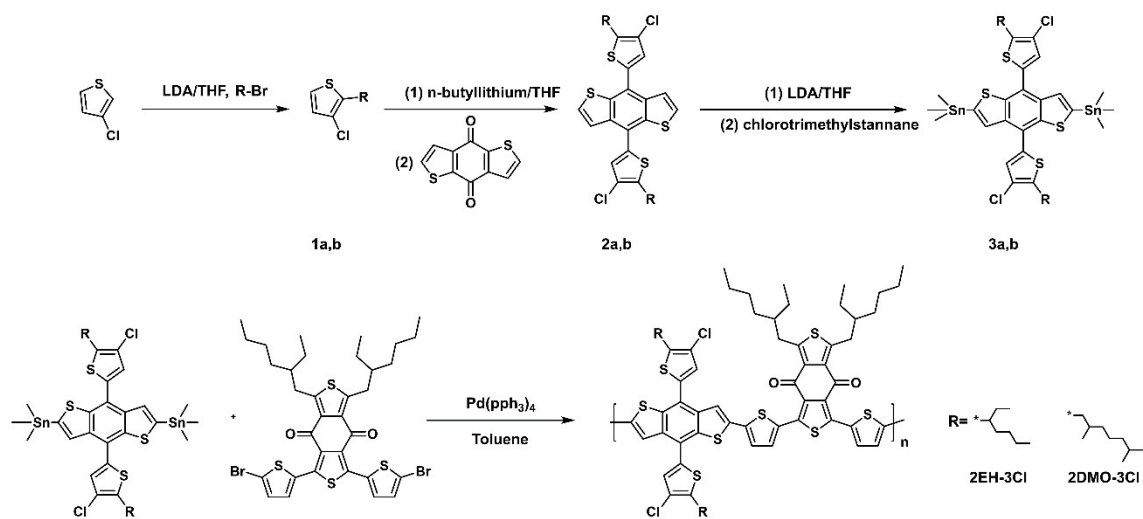
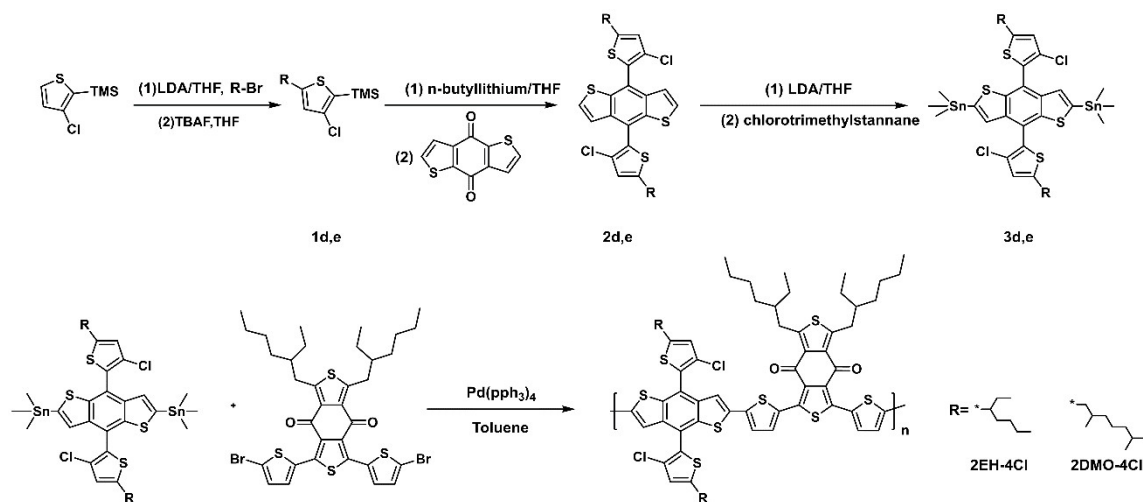


Figure S23. Device shlef-lifetime under the LED lighting of PBDB-DMO-4Cl:Y6 based device.



Scheme S1. Synthetic scheme for PBDB-EH-3Cl and PBDB-DMO-3Cl.



Scheme S2. Synthetic scheme for PBDB-EH-4Cl and PBDB-DMO-4Cl.

Table S1. List of renewable power sources along with a capacity of harvested power.

Power sources	Type	Transducers	Typical harvested power density	Ref
Solar	Electromagnetic	Solar Panels (outdoors) (0-200 k lux)	$\sim 15 \text{ mW/cm}^2$	S1
Indoor lights	Electromagnetic	Solar Panels (indoors) (1-3 k lux)	$\sim 15 \text{ }\mu\text{W/cm}^2$	S2
Thermal	Thermal	Thermoelectric generators (TEG)	$\sim 15 \text{ }\mu\text{W/cm}^2$	S3
Vibration	Mechanical	Piezoelectric generators	$\sim 330 \text{ }\mu\text{W/cm}^2$	S4
		Electrostatic generators	$\sim 50 \text{ }\mu\text{W/cm}^2$	S5
RF	Electromagnetic	Antenna	$\sim 12 \text{ nW/cm}^2$	S6

References

[S1] M. Hassanaliyagh, T. Soyata, A. Nadeau, and G. Sharma, "UR-SolarCap: An open source intelligent auto-wakeup solar energy harvesting system for supercapacitor based energy buffering," *IEEE Access*, vol. 4, pp. 542–557, Mar. 2016.

[S2] Y. K. Tan and S. K. Panda, "Energy harvesting from hybrid indoor ambient light and thermal energy sources for enhanced performance of wireless sensor nodes," *IEEE Trans. Ind. Electron.*, vol. 58, no. 9, pp. 4424–4435, 2011.

[S3] X. Lu and S.-H. Yang, "Thermal energy harvesting for WSNs," in *Proc. IEEE Int. Conf. Systems, Man and Cybernetics*, pp. 3045–3052, 2010.

[S4] D. L. Churchill, M. J. Hamel, C. P. Townsend, and S. W. Arms, "Strain energy harvesting for wireless sensor networks," *Smart Struct. Mater.*, vol. 5055, pp. 319–327, 2003.

[S5] S. Boisseau, G. Despesse, and A. Sylvestre, "Optimization of an electret-based energy harvester," *Smart Mater. Struct.*, vol. 19, no. 7, pp. 075015, 2010.

[S6] M. Piñuela, P. D. Mitcheson, and S. Lucyszyn, "Ambient RF energy harvesting in urban and semi-urban environments," *IEEE Trans. Microwave Theory Tech.*, vol. 61, no. 7, pp. 2715–2726, July 2013.

Table S2. UV-vis data and energy level for PM7 series polymer

Donor	<i>Mn</i> (pdi) [kDa]	λ_{max}^{sol} [nm] ^(a)	λ_{max}^{film} [nm] ^(b)	E_g^{opt} [eV] ^(c)	HOMO [eV] ^(d)	λ_{max}^{sol} [eV] ^(d)
PBDB-EH-3CI	26 (1.9)	609	614	1.82	-5.33	-3.51
PBDB-EH-4CI	20 (2.2)	607	615	1.82	-5.34	-3.52
PBDB-DMO-3CI	32 (2.3)	607	612	1.82	-5.35	-3.53
PBDB-DMO-4CI	30 (2.2)	612	621	1.83	-5.36	-3.53

^a λ_{max} values of corresponding chloroform solutions. ^b λ_{max} values of corresponding thin-films spin-coated from chloroform solutions. ^cOptical bandgaps calculated from the absorption onsets. ^dabsorption coefficients at the λ_{max} s estimated from film absorption spectra. ^dHOMO energy levels were estimated from cyclic voltammetry: E_{HOMO} (eV) = $-(E_{onset}^{ox} - E_{onset}^{Fc/Fc^+}) + E_{HOMO}^{Fc}$; $E_{onset}^{Fc/Fc^+} = 0.46$ eV, $E_{HOMO}^{Fc} = -4.8$ eV, E_{LUMO} (eV) = E_{HOMO} (eV) - E_g^{opt} (eV).

Table S3. Summary of recently reported photovoltaic performance under halogen lamp 1000 lx illumination.

Photoactive layer	V_{oc} (mV)	J_{sc} ($\mu A/cm^2$)	FF (%)	P_{max} ($\mu W/cm^2$)	ref
PBDB-T:IDIC	710	202.7	65.0	94.1	[1]
PBDB-T:IDICO1	770	252.4	66.0	102.1	[1]
PBDB-T:IDICO2	770	271.2	63.0	141.4	[1]
PM6:Y6	720	454.2	77.7	254.1	[2]
PM7:IT-4F	750	309.8	72.6	168.7	[2]
PTB7-Th:IEICO-4F	630	403.2	69.8	177.3	[2]
PBDB-T:BTA3	1050	289.2	52.4	159.1	[3]
PBDB-TF:BTA3	1140	180.4	54.3	111.7	[3]
PBDB-TCI:BTA3	1180	138.2	43.6	71.1	[3]
PDTBTBz-2F _{anti} :PC ₇₁ BM	809	116.8	70.2	66.3	[4]
P3HT:PC ₇₁ BM	486	71.8	71.0	24.8	[4]
PBDB-T:PC ₇₁ BM	669	108.3	71.0	51.4	[4]
PTB7:PC ₇₁ BM	576	171.4	67.4	66.5	[4]

(1) Synthesis of 2-alkyl-3-chloro-thiophene (1a,1b)

To a solution of 3-chlorothiophene (10 g, 84.7 mmol) in anhydrous THF (50 mL) at -78°C was added LDA (42.4 mL, 84.7 mmol, 2 M in THF) under nitrogen atmosphere. The mixture was stirred at -78°C for 2 hours, alkyl bromide (84.7 mmol) was added dropwise into the flask and then the mixture was elevated to the temperature slowly to room temperature overnight. The reaction mixture was poured into water and extracted with diethyl ether and then dried over anhydrous MgSO₄. The crude product was obtained through vacuum distillation and used directly for next step without further purification.

(2) Synthesis of 2-alkyl-3-chloro-thiophene-BDT (2a,2b)

To a solution of 2-alkyl-3-chloro-thiophene (20 mmol) in anhydrous THF (150 mL) at -0°C was added LDA (10 mL, 20 mmol, 2 M in THF) under nitrogen atmosphere, After stirring for 2 hours, Benzo[1,2-b:4,5-b']dithiophene-4,8-dione (1.76 g, 8 mmol) was added into the flask and stirred at 60°C for 5 hours. After cooling to room temperature, a solution of SnCl₂•2H₂O (4.2 g, 20 mmol) in 10% HCl was added and stirred overnight. The mixture was poured into ice water and extracted with diethyl ether, the organic phase was dried over anhydrous MgSO₄ and removed solvent. The crude product was purified by silica gel chromatography using hexane as an eluent to afford the product as a yellow solid.

2a: EH-3Cl-BDT (3.0 g, yield 53%), ¹H NMR matched well with previous report^[S1].

2b: DMO-3Cl-BDT (3.2 g, yield 58%), ¹H NMR (300 MHz, CD₂Cl₂) δ 7.61 (d, J = 5.7 Hz, 2H), 7.52 (d, J = 5.7 Hz, 2H), 7.25 (s, 2H), 2.95 – 2.88 (m, 4H), 1.82 – 1.71 (m, 2H), 1.62 – 1.49 (m, 6H), 1.41 – 1.15 (m, 12H), 0.99 (d, J = 6.3 Hz, 6H), 0.89 (d, J = 6.6 Hz, 12H). ¹³C NMR (125 MHz, CDCl₃) δ 139.67, 139.16, 136.66, 135.72, 128.25, 128.16, 123.42, 123.19, 122.02, 39.43, 37.85, 37.13, 32.65, 28.13, 25.79, 24.85, 22.88, 22.80, 19.70. HRMS (EI, m/z): calcd. for C₃₈H₄₈Cl₂S₄, 702.2016, found, 702.

(3) Synthesis of 2-alkyl-3-chloro-thiophene-BDT-Sn (3a,3b)

To a solution of 2-alkyl-3-chloro-thiophene-BDT (10 mmol) in anhydrous THF (50 mL) at -78°C was added LDA (12.5 mL, 25 mmol, 2 M in THF) under nitrogen atmosphere, after stirring for 3 hours, trimethyltin chloride solution (25 ml, 25 mmol, 1M in THF) was added into the flask and stirred at 25°C overnight. The mixture was poured into water and extracted with diethyl ether, the organic phase was dried over anhydrous MgSO₄ and removed solvent. The crude product was purified by recrystallization from methanol to afford product as yellow solid.

3a: EH-3Cl-BDT-Sn (3.3 g, yield 55%), ¹H NMR matched well with previous report. ^[S1]

3b: DMO-3Cl-BDT-Sn (3.4 g, yield 54%), ¹H NMR (300 MHz, CD₂Cl₂) δ 7.65 (s, 2H), 7.25 (s, 2H), 2.93 (m, 4H), 1.78 (m, 2H), 1.66 – 1.49 (m, 6H), 1.42 – 1.13 (m, 12H), 1.00 (d, J = 6.3

Hz, 6H), 0.88 (d, J = 6.6 Hz, 12H), 0.42 (s, 18H). ¹³C NMR (125 MHz, CDCl₃) δ 143.48, 143.36, 139.30, 137.47, 136.48, 130.75, 128.05, 121.87, 121.70, 39.45, 37.82, 37.15, 32.70, 28.12, 25.82, 24.86, 22.88, 22.80, 19.70, -8.11. HRMS (EI, m/z): calcd. for C₄₄H₆₄Cl₂S₄Sn₂, 1030.1312, found, 1030.

(4) Synthesis of 2-alkyl-4-chloro-thiophene (1d,1e)

To a solution of (3-chlorothiophen-2-yl)trimethylsilane (16 g, 84.7 mmol) in anhydrous THF (50 mL) at -78°C was added LDA (42.4 mL, 84.7 mmol, 2 M in THF) under nitrogen atmosphere. The mixture was stirred at -78°C for 2 hours, alkyl bromide (84.7mmol) was added dropwise into the flask and then the mixture was elevated to the temperature slowly to room temperature overnight. The reaction mixture was poured into water and extracted with diethyl ether and then dried over anhydrous MgSO₄. The crude product was obtained through vacuum distillation and used directly for the next step without further purification.

(5) Synthesis of 2-alkyl-4-chloro-thiophene-BDT (2d,2e)

To a solution of 2-alkyl-4-chloro-thiophene (20 mmol) in anhydrous THF (150 mL) at -0°C was added LDA (10 mL, 20 mmol, 2 M in THF) under nitrogen atmosphere, After stirring for 2 hours, Benzo[1,2-b:4,5-b']dithiophene-4,8-dione (1.76 g, 8 mmol) was added into the flask and stirred at 60 °C for 5 hours. After cooling to room temperature, a solution of SnCl₂•2H₂O (4.2 g, 20 mmol) in 10% HCl was added and stirred overnight. The mixture was poured into ice water and extracted with diethyl ether, the organic phase was dried over anhydrous MgSO₄ and removed solvent. The crude product was purified by silica gel chromatography using hexane as an eluent to afford the product as a yellow solid.

2d: EH-4Cl-BDT (3.1 g, yield 60%), ¹H NMR (300 MHz, CD₂Cl₂) δ 7.60 (d, J = 5.7 Hz, 2H), 7.53 (d, J = 5.7 Hz, 2H), 7.24 (d, J = 1.6 Hz, 2H), 2.85 (d, J = 7.0 Hz, 4H), 1.76 (q, J = 6.2 Hz, 2H), 1.51 – 1.27 (m, 16H), 0.95 (m, 12H). ¹³C NMR (125 MHz, CDCl₃) δ 139.16, 138.48, 136.65, 136.04, 128.19, 128.15, 123.42, 123.17, 122.86, 41.07, 32.66, 32.21, 28.97, 25.97, 23.15, 14.27, 11.01. HRMS (EI, m/z): calcd. for C₃₄H₄₀Cl₂S₄, 646.1390, found, 646.

2e: DMO-4Cl-BDT (3.5 g, yield 66%)¹H NMR (300 MHz, CD₂Cl₂) δ 7.61 (d, J = 5.7 Hz, 2H), 7.54 (d, J = 5.7 Hz, 2H), 7.25 (s, 2H), 2.98 – 2.85 (m, 4H), 1.78 (m, 2H), 1.65 – 1.49 (m, 6H), 1.44 – 1.13 (m, 12H), 0.99 (d, J = 6.3 Hz, 6H), 0.88 (d, J = 6.6 Hz, 12H). ¹³C NMR (300 MHz, CDCl₃) δ 139.69, 139.18, 136.68, 135.74, 128.27, 128.18, 123.44, 123.21, 122.04, 39.45, 37.87, 37.15, 32.67, 28.15, 25.81, 24.87, 22.90, 22.82, 19.72. HRMS (EI, m/z): calcd. for C₃₈H₄₈Cl₂S₄, 702.2016, found, 702.

(6) Synthesis of 2-alkyl-4-chloro-thiophene-BDT-Sn (3d,3e)

To a solution of 2-alkyl-4-chloro-thiophene-BDT (5 mmol) in anhydrous THF (50 mL) at -78°C was added LDA (6 mL, 12 mmol, 2 M in THF) under nitrogen atmosphere after stirring for 3 hours, trimethyltin chloride solution (15 ml, 15 mmol, 1M in THF) was added into the flask and stirred at 25°C overnight. The mixture was poured into water and extracted with diethyl ether, the organic phase was dried over anhydrous MgSO₄ and removed solvent. The crude product was purified by recrystallization from methanol to afford product as yellow solid.

3d: EH-4Cl-BDT-Sn (2.4 g, 50%), ¹H NMR (300 MHz, CD₂Cl₂) δ 7.66 (s, 2H), 7.26 (s, 2H), 2.86 (d, J = 7.0 Hz, 4H), 1.75 (m, 2H), 1.51 – 1.27(m, 16H), 0.99 – 0.83 (m, 12H), 0.41 (s, 18H). ¹³C NMR (125 MHz, CDCl₃) δ 143.48, 143.37, 138.10, 137.44, 136.80, 130.74, 127.90, 122.68, 121.68, 41.01, 32.67, 32.27, 28.99, 26.05, 23.18, 14.30, 11.07, -8.16. HRMS (EI, m/z): calcd. for C₄₀H₅₆Cl₂S₄Sn₂, 974.0686, found, 974.

3e: DMO-4Cl-BDT-Sn (2.8 g, 62%), ¹H NMR (300 MHz, CD₂Cl₂) δ 7.65 (s, 2H), 7.26 (s, 2H), 3.11 – 2.73 (m, 4H), 1.80 (m, 2H), 1.66 – 1.47 (m, 6H), 1.46 – 1.12 (m, 12H), 1.00 (d, J = 6.3 Hz, 6H), 0.88 (d, J = 6.6 Hz, 12H), 0.42 (s, 18H). ¹³C NMR (125 MHz, CDCl₃) δ 143.36, 139.30, 137.46, 136.48, 130.75, 128.04, 121.88, 121.70, 39.45, 37.82, 37.15, 32.69, 28.12, 25.82, 24.86, 22.89, 22.80, 19.70, -8.10.

HRMS (EI, m/z): calcd. for C₄₄H₆₄Cl₂S₄Sn₂, 1030.1312, found, 1030.

(7) Synthesis of PBDB-EH-3Cl and PBDB-DMO-3Cl.

2-alkyl-3-chloro-thiophene-BDT-Sn (0.1 mmol), 1,3-bis(5-bromothiophen-2-yl)-5,7-bis(2-ethylhexyl)-4H,8H-benzo[1,2-c:4,5-c']dithiophene-4,8-dione(77mg, 0.1mmol), and Pd(pph₃)₄ (5.8mg, 0.005mmol) were combined in a 10 mL two-necked flask. Anhydrous toluene (5 mL) was added under the argon atmosphere. The mixture was reacted 24 hrs at 110 °C after cooled down, then the reactant mixture was poured into methanol (200 mL) for precipitation. The precipitate was filtered and Soxhlet extracted with methanol, hexane, and chloroform. The ingredient extracted from chloroform was concentrated, precipitated into 200 mL methanol, filtered, and dried under vacuum to give the dark solid.

PBDB-EH-3Cl (80 mg, 67%). (M_n= 27 KDa, PDI= 1.9)

PBDB-DMO-3Cl (90 mg, 70%). (M_n= 32 KDa, PDI= 2.3)

¹H NMR (300 MHz, CDCl₃): δ (ppm) 7.70 – 6.68 (broad, 8H), 3.15 – 2.70(broad, 8H), 1.91–0.45 (broad, 68H).

(8) Synthesis of PBDB-EH-4Cl, and PBDB-DMO-4Cl.

2-alkyl-4-chloro-thiophene-BDT-Sn (0.1 mmol), 1,3-bis(5-bromothiophen-2-yl)-5,7-bis(2-ethylhexyl)-4H,8H-benzo[1,2-c:4,5-c']dithiophene-4,8-dione(77mg, 0.1mmol), and Pd(pph₃)₄ (5.8mg, 0.005mmol) were combined in a 10 mL two-necked flask. Anhydrous toluene (5 mL)

was added under the argon atmosphere. The mixture was reacted 24 hrs at 110 °C after cooled down, then the reactant mixture was poured into methanol (200 mL) for precipitation. The precipitate was filtered and Soxhlet extracted with methanol, hexane, and chloroform. The ingredient extracted from chloroform was concentrated, precipitated into 200 mL methanol, filtered, and dried under vacuum to give the dark solid.

PBDB-EH-4Cl (90 mg, 71%). (M_n = 20 KDa, PDI= 2.2)

$^1\text{H NMR}$ (300 MHz, CDCl_3): δ (ppm) 7.67 – 6.80 (broad, 8H), 3.06 – 2.68(broad, 8H), 1.91–0.45 (broad, 60H).

PBDB-DMO-4Cl (93 mg, 71%). (M_n = 30 KDa, PDI= 2.2)

$^1\text{H NMR}$ (300 MHz, CDCl_3): δ (ppm) 7.70 – 6.68 (broad, 8H), 3.15 – 2.72(broad, 8H), 1.90–0.46 (broad, 68H).

References

- [S0] Zhang, S., Qin, Y., Zhu, J. and Hou, J., 2018. Over 14% efficiency in polymer solar cells enabled by a chlorinated polymer donor. *Advanced Materials*, 30(20), p.1800868.
- [1] H. S. Ryu, H. G. Lee, S. C. Shin, J. Park, S. H. Kim, E. J. Kim, T. J. Shin, J. W. Shim, B. J. Kim, H. Y. Woo, *J. Mater. Chem. A* **2020**, 8, 23894.
- [2] Z. Chen, H. Yin, Z. Wen, S. K. So, X. Hao, *Sci. Bull.* **2021**, 66, 1648.
- [3] Z. Chen, T. Wang, Z. Wen, P. Lu, W. Qin, H. Yin, X. T. Hao, *ACS Energy Lett.* **2021**, 6, 3203.
- [4] Y. J. You, C. E. Song, Q. V. Hoang, Y. Kang, J. S. Goo, D. H. Ko, J. J. Lee, W. S. Shin, J. W. Shim, *Adv. Funct. Mater.* **2019**, 29, 1.